International Journal of Sciences and Techniques of Automatic control & computer engineering
IJ-STA, Special Issue, CEM, December 2008, pp. 548–565.

Power Flow Control and VAR Compensation in a Doubly Fed induction Generator

Kamel Jemli [*], Mohamed Jemli [*] , Moncef Gossa [*]
Mohamed Boussak[**]

[*] *Unit of research C3S*
Ecole Supérieure des Sciences et Techniques de Tunis (ESSTT)
5 Avenue Taha Hussein – BP 56, Bab Mnara – 1008 Tunis

kamel.jemli@isetzg.rnu.tn, mohamed.jemli@isetr.rnu.tn, moncef.gossa@esstt.rnu.tn

[**] *Laboratoire des Sciences de l'Information et des Systèmes (LSIS), UMR CNRS 616*
8 – Ecole Centrale Marseille (ECM) – 13451 Marseille Cedex 20 – France

Email : mohamed.boussak@ec-marseille.fr

Abstract. This paper deals with the indirect control of the Doubly Fed Induction generator (DFIG). In order to control the power flow between the DFIG and the electrical grid, we present a control strategy which will enable the optimization of the power injected into the network, the identification and compensation of the harmonics as well as the compensation of the reactive power.

Keywords: Wind turbine, Doubly fed induction generator, Power flow control, Reactive power compensation, Harmonics active filtering.

1. Introduction

During the last years the productions of electrical energy from wind energy have increased. Several power plants have been put in production everywhere in the world. The interest focused on this type of energy is due to the importance of this source of power in term of quantity of energy and its environmental impact. In the wind power stations, the induction machines are used as generators [1]. In this study we will develop a control strategy of the Doubly Fed Induction Generator (D.F.I.G) which offers, compared to other types of generator some advantages as:

- The possibility of following the optimum of the power provided by the wind-turbine (a slip which can vary until 40%).

This paper was recommended for publication in revised form by the editor Staff.
Edition: CPU of Tunis, Tunisia, ISSN: 1737-7749

- The control of the power provided by the generator using converters dimensioned with 20 to 30% of the nominal power of the generator
- Low cost
- Robustness
- Reduction of the fluctuations in the power provided to the network
- Reduction of the mechanical constraints
- Possibility of controlling the power-factor.

D.F.I.G is composed of a wound rotor induction generator and an Unified Power Flow Controllers (UPFC) composed by two controlled inverters C_{Grid} and C_{Rot}. The generator's stator is directly connected to the network, by there it provides to the electric grid the major quantity of electric power converted from the wind power; the remainder (about 25%) is conveyed through the rotor, connected to the network using an UPFC (fig.1). This type of topology was the subject of several researches; the obtained results show that owing to the UPFC control we can drive the D.F.I.G. In fact , the control of C_{Rot} permits as to act on the total power provided to the electric grid; [2] [3] Whereas, the control of the C_{Grid} converter makes possible to control the continuous bus voltage and to compensate the reactive power needed by the stator circuit.[7]
The first part of this study consists on the presentation of the dynamic DFIG model then, we will establish the control strategies of the UPFC. Finally, we deal with the harmonics, due to the presence of the power electronics, in order to quantify the harmonic rate distortion and to propose a control strategy allowing the identification and the instantaneous compensation of the harmonics and the reactive power.

2. Model of the asynchronous wound rotor generator

The electric equations of the doubly fed induction generator in the d-q synchronously reference frame are [6]:

$$\overline{V_s} = \left[R_s + (p + j\omega_s)L_s\right]\overline{i_s} + (p + j\omega_s)L_m\overline{i_r} \tag{1}$$

$$\overline{V_r} = (p + jg\omega_s)L_m\overline{i_s} + \left[R_r + (p + jg\omega_s)L_r\right]\overline{i_r} \tag{2}$$

with:

$$\begin{cases} \overline{V_s} = V_{sd} + jV_{sq} \\ \overline{V_r} = V_{rd} + jV_{rq} \\ \overline{i_s} = i_{sd} + ji_{sq} \\ \overline{i_r} = i_{rd} + ji_{rq} \\ L_s = L_{ss} + L_m \\ L_r = L_{rs} + L_m \end{cases} \tag{3}$$

$$\begin{bmatrix} V_d \\ V_q \end{bmatrix} = \frac{2}{3}\begin{bmatrix} \cos\theta_{s,r} & \cos(-\theta_{s,r} + \frac{2\pi}{3}) & \cos(-\theta_{s,r} - \frac{2\pi}{3}) \\ s\sin(-\theta_{s,r}) & \sin(-\theta_{s,r} + \frac{2\pi}{3}) & \sin(-\theta_{s,r} - \frac{2\pi}{3}) \end{bmatrix}\begin{bmatrix} V_a \\ V_b \\ V_c \end{bmatrix} \tag{4}$$

The index s is relative to the stator transformation and the index r is relative to the rotor transformation.

$\theta_s = \int \omega_s dt = \omega_s t$ For a constant frequency of the stator currents

$\theta_r = \int (\omega_s - \omega_r) dt$ and $\frac{d\theta_r}{dt} = \omega_s - \omega_r = g.\omega_s$ (5)

The mechanical equation of the generator is:

$$J\frac{d\omega_r}{dt} = np(T_m - T_e) \quad (6)$$

$$T_e = \frac{3}{2} npL_m\left(i_{sq}i_{rd} - i_{sd}i_{rq}\right) \quad (7)$$

with:

T_m: Mechanical torque
T_e: Electromagnetic Torque
n_p: number of poles pairs
J: Effective inertia of the revolving part

Using the equations [1] and [2] we lead to the next system of equations:

$$\begin{cases} \frac{di_{sd}}{dt} = \frac{1}{L_s}\left[V_{sd} - R_s i_{sd} - L_m \frac{di_{rd}}{dt} + L_s\omega_s i_{sq} + L_m\omega_s i_{rq}\right] \\ \frac{di_{sq}}{dt} = \frac{1}{L_s}\left[V_{sq} - R_s i_{sq} - L_m \frac{di_{rq}}{dt} + L_s\omega_s i_{sq} - L_m\omega_s i_{rd}\right] \\ \frac{di_{rd}}{dt} = \frac{1}{L_r}\left[V_{rd} - R_r i_{rd} - L_m \frac{di_{sd}}{dt} + L_r\omega_s g i_{rq} + L_m g\omega_s i_{sq}\right] \\ \frac{di_{rq}}{dt} = \frac{1}{L_r}\left[V_{rq} - R_r i_{rq} - L_m \frac{di_{sq}}{dt} - L_r\omega_s g i_{rd} - L_m g\omega_s i_{sd}\right] \end{cases} \quad (8)$$

where

R_s: resistance of the stator phase
R_r: resistance of the rotor phase
L_s: cyclic inductance of the stator phase
L_r: cyclic inductance of the rotor phase
L_m: maximum mutual inductance Stator-rotor

3. Doubly Fed Asynchronous generator

A doubly fed induction generator can deliver the power not only from the stator but also from the rotor. It has also the capacity to deliver the electric power with voltage and frequency constants for a variation of the speed of ± 20 to 40% around the synchronous speed. [4].

This study is focused on the improvement of the UPFC performances.

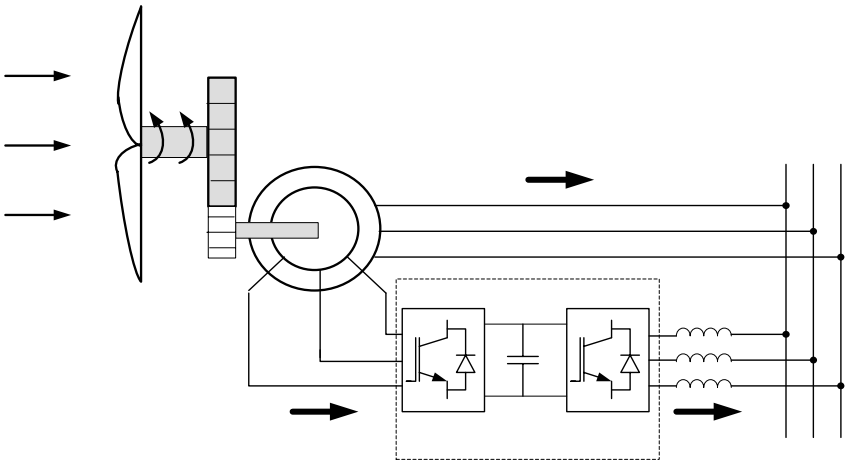

Fig. 1. Doubly Fed Induction Generator (DFIG).

The mechanical power and the stator electric power are expressed as follows:

$P_m = T_m \Omega_r$ (9)

$P_s = T_e \, \Omega_s$ (10)

In steady state and at fixed speed;

$T_m = T_e$ and $P_m = P_s + P_r$ (11)

$P_r = P_m - P_s = T_m.\Omega_r - T_e.\Omega_s = - T_m (\Omega_r - \Omega_s) = - g.P_s$ (12)

Where g designs the slip of the generator

4. Control strategy of the DFIG

In this part, it is necessary to establish the control strategy of the two converters C_{rot} and C_{grid} (respectively converter side rotor and grid side converter) as well as the angle of orientation of pale (pitch angle). The two converters (C_{grid} and C_{rot}) can control the active power of the turbine, the voltage of the continuous bus and the reactive power.

4.1. Control of the side rotor converter C_{rot}

We choose a synchronously rotating reference frame so that the d-axis thus coincides with the desired direction of stator flux; hence, we will have:

$$\psi_{ds} = \psi_s = L_s i_{ds} + L_m i_{dr} \quad (13)$$

$$\psi_{qs} = L_s i_{sq} + L_m i_{rq} = 0 \quad (14)$$

The electromagnetic Torque will be reduced to:

$$T_e = n_p \frac{L_m}{L_s}\left(\psi_{ds} i_{qr}\right) \tag{15}$$

By neglecting resistances of the stator phases the stator voltage will be expressed by:

$$v_s \approx \frac{d\psi_s}{dt} \tag{16}$$

We can also deduce

$v_{ds} = 0$

and

$v_{qs} = v_s = \omega_s \psi_{ds}$

The equations [13] and [14] give these next expressions of the "d" and "q" stator currents:

$$i_{ds} = \frac{\psi_{ds}}{L_s} - \frac{L_m}{L_s} i_{dr} \tag{17}$$

$$i_{qs} = -\frac{L_m}{L_s} i_{qr} \tag{18}$$

We lead to an uncoupled power control; where, the transversal component i_{qr} of the rotor current controls the active power. The reactive power is imposed by the direct component i_{dr}.

$$P = -v_s \frac{L_m}{L_s} i_{qr} \tag{19}$$

$$Q = \frac{v_s \psi_{ds}}{L_s} - \frac{v_s L_m}{L_s} i_{dr} \tag{20}$$

The arrangement of the equations gives the expressions of flux and the voltages according to the rotor currents:

$$\begin{cases} \psi_{dr} = \left(L_r - \dfrac{L_m^2}{L_s}\right) i_{dr} + \dfrac{L_m v_s}{\omega_s L_s} \\ \psi_{qr} = \left(L_r - \dfrac{L_m^2}{L_s}\right) i_{qr} \end{cases} \tag{21}$$

$$\begin{cases} v_{dr} = R_r i_{dr} + \left(L_r - \dfrac{L_m^2}{L_s}\right)\dfrac{di_{dr}}{dt} - g\omega_s\left(L_r - \dfrac{L_m^2}{L_s}\right) i_{qr} \\ v_{qr} = R_r i_{qr+}\left(L_r - \dfrac{L_m^2}{L_s}\right)\dfrac{di_{qr}}{dt} - g\omega_s\left(L_r - \dfrac{L_m^2}{L_s}\right) i_{dr} + g\omega_s \dfrac{L_m^2 v_s}{\omega_s L_s} \end{cases} \tag{22}$$

Note by:

$$\sigma = 1 - \frac{L_m^2}{L_s.L_r}$$

$e1 = -g.\omega_s.\sigma.L_r.i_{qr}$

$e2 = g.L^2_m v_s/L_s - g.\omega_s.\sigma.L_r.i_{dr}$

Then we obtain the next transfer function:

$$i_{rd}(P) = \frac{1/R_r}{1+\frac{L_r.\sigma}{R_r}P}[v_{rd}(P) - e1(P)] \tag{23}$$

$$i_{rq}(P) = \frac{1/R_r}{1+\frac{L_r.\sigma}{R_r}P}[v_{rq}(P) - e2(P)] \tag{24}$$

The next figure shows the closed loop system using a rotor current regulation with a PI controller.

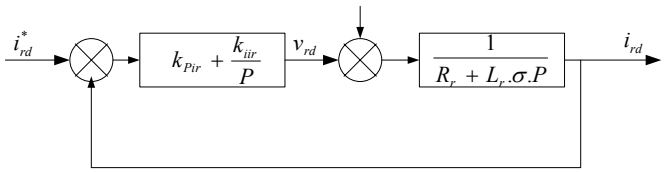

Fig. 2. Rotor current regulator diagram block.

Where K_{pir} and K_{iir} denote proportional and integral gains of the, *d-q* axis current, (PI) controller.

Fig. 5. Closed loop transfer function.

G(P) is the closed loop transfer function.

$$G(P) = \frac{\frac{K.K_{iir}}{\tau}\left(1 + \frac{K_{pir}}{K_i}P\right)}{P^2 + P\left(\frac{1+K.K_{pir}}{\tau}\right) + \frac{K.K_{iir}}{\tau}} \quad (25)$$

$K = \frac{1}{R_r}$ is a gain and $\tau = \sigma.\frac{L_r}{R_r}$ is a time constant.

This equation can be assimilate to a second order transfer function

$$G_{CLS} = \frac{\omega_0^2(1 + \frac{K_{pir}}{K_{iir}}P)}{P^2 + 2\xi\omega_0 P + \omega_0^2} \quad (26)$$

Where

$$\begin{cases} \omega_0 = \sqrt{\frac{K.K_{iir}}{\tau}} \\ \xi = \frac{1 + K.K_{pir}}{2\omega_0\tau} \end{cases}$$

ω_0 and ξ denote natural frequency and damping ratio, respectively.

The optimal response is obtained for $\xi = 0,7 \Rightarrow \omega_0.t_r = 3$.

By choosing a system response time (tr) we can deduce K_{iir} and K_{pir} (PI regulator coefficients).

$\omega_0 = 3/t_r$

$$\boxed{K_{iir} = \frac{\omega_0^2.\tau}{K}}$$

$$\boxed{K_{pir} = \frac{\xi.2\omega_0\tau - 1}{K}}$$

4.2. Control of the grid side converter C_{Grid}

The two essential functions of the grid side converter are:

- To maintain a fixed voltage at the boundaries of the capacitor
- To compensate the reactive power consumed by the induction generator

For that, a control strategy, can determine the direct and transversal components of the current delivered by C_{grid}. The direct component of this current acts on the continuous bus voltage whereas, the transversal component acts on the quantity of reactive power.

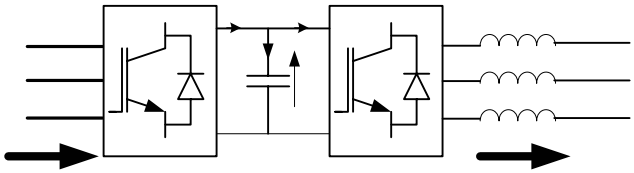

Fig 4. Unified Power Flow Controllers (UPFC).

$$i_C = C.\frac{dV_{DC}}{dt} = i_{CRot} - i_{CGrid} \tag{27}$$

$$C.V_{DC}.\frac{dV_{DC}}{dt} = P_{CRot} - P_{CGrid} \tag{28}$$

With: $P_{CRot} = g.P_S$

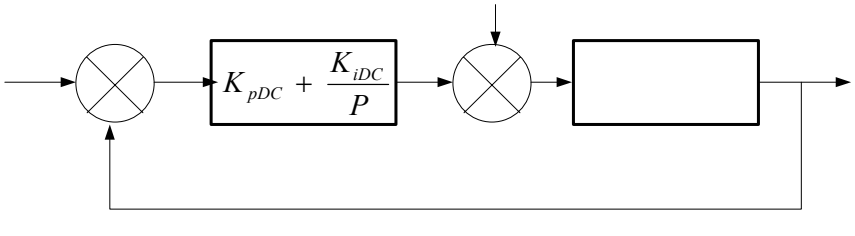

Fig. 5. Continuous bus voltage Regulation block diagram.

Where K_{pDC} and K_{iDC} denote proportional and integral gains of the, continuous bus, (PI) controller.
F(p) is the transfer function deduced from the equation [27]:

$$F(p) = \frac{1}{C.P}$$

Note by G_{DC} the closed loop transfer function.

$$G_{DC} = \frac{\frac{K_{iDC}}{C}\left(\frac{K_{pDC}}{K_{iDC}}P + 1\right)}{P^2 + \frac{K_{pDC}}{C}P + \frac{K_{iDC}}{C}} \tag{29}$$

This equation can be assimilate to a second order transfer function

$$G_{CLS} = \frac{\omega_0^2(1 + \frac{K_{pDC}}{K_{iDC}}P)}{P^2 + 2\xi\omega_0 P + \omega_0^2} \tag{30}$$

So we can deduce the regulator parameter:

$$\boxed{K_{iDC} = \omega_0^2 .C} ; \boxed{K_{pDC} = 2\,\omega_0 .\xi .C}$$

Where ω_0 and ξ denote natural frequency and damping ratio, respectively.

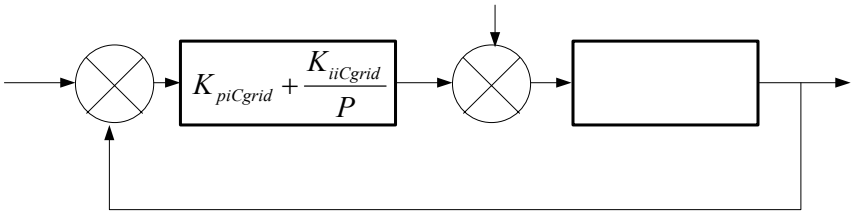

Fig. 6. C_{grid} Converter current Regulation block diagram.

F_f (P) is the filter (R_f , L_f) transfer function

$$F_f = \frac{1}{R_f + L_f .P} \tag{31}$$

The closed loop transfer function, G_{iCgrid}, is given by the following expression:

$$G_{iCgrid} = \frac{\frac{K_{iiCgrid}}{L_f}\left(1 + \frac{K_{piCgrid}}{K_{iiCgrid}}P\right)}{P^2 + \left(\frac{R_f + K_{piCgrid}}{L_f}\right)P + \frac{K_{iiCgrid}}{L_f}} = \frac{\omega_0^2\left(1 + \frac{K_{piCgrid}}{K_{iiCgrid}}P\right)}{P^2 + 2\xi\omega_0 P + \omega_0^2} \tag{32}$$

Then we can deduce the PI regulator coefficient ($K_{piCgrid}$, $K_{iiCgrid}$):

$\boxed{K_{piCgrid} = 2.L_f.\xi.\omega_0 - R_f}$; $\boxed{K_{iiCgrid} = L_f.\omega_0^2}$

where:

V_{DC}: voltage of the continuous Bus
I_{Cgrid}: Current delivered by the grid side converter
V_{CGrid}: Voltage of the grid side converter
V_{grid}: Stator voltage (Grid voltage)
L_f: Smoothing bobbin self inductance
R_f: Smoothing bobbin resistance
ω_s: Stator pulsation
*: reference value

4.3. Simulation results

For simulation, we used an asynchronous wound rotor machine, whose parameters are quoted in appendix. This machine is coupled with a wind turbine 15kW; Initially The wind speed is equal to 12m/s, at the moment t=2s the wind speed passes from 12m/s to 10 m/s then from 10 m/s to 11 m/s at the moment t=3.3s.

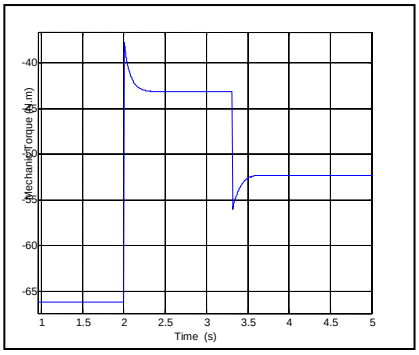

Fig. 7. Mechanical torque provided by the wind turbine.

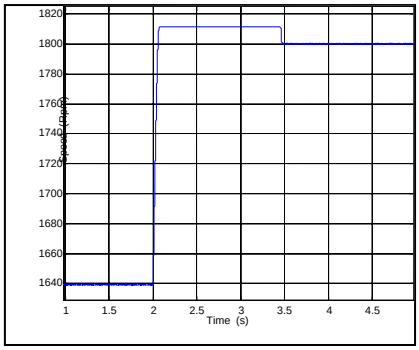

Fig. 8. Generator speed.

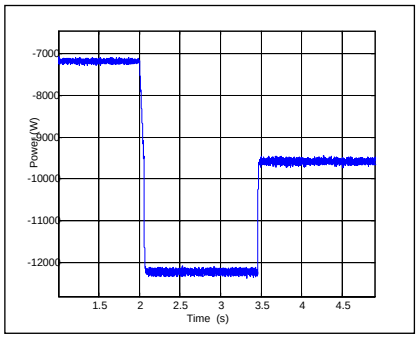

Fig. 9. Active power provided to the grid.

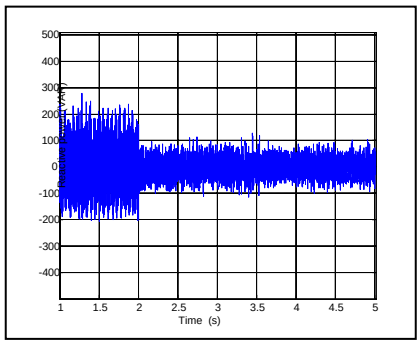

Fig. 10. Reactive power on the grid side.

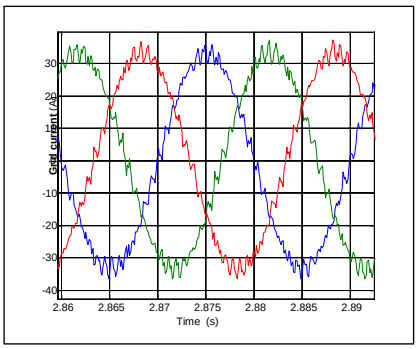

Fig. 11. Three phase grid current.

It is noticed that the control satisfied several criteria such as the regulation of the continuous bus voltage V_{DC}, the compensation of the reactive power, a good stability of speed. Nevertheless, this control presents a major disadvantage which is expressed by a high rate of harmonic distortion (7% to 13% according to the speed of the wind applied). This is due to the power electronics equipments used in the UPFC.

Table 1: Rate of Harmonic Distortion for various speeds of the wind

v (m/s)	10	12	11
THD (%)	12,8	7,1	9,26

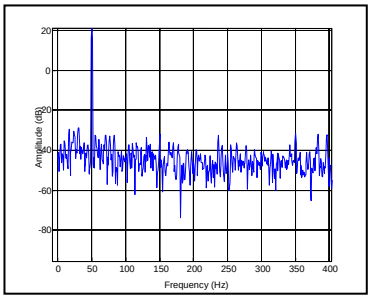

Fig. 12. Frequency distribution of the line current.

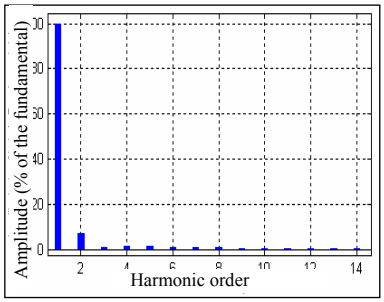

Fig.13. spectral concentration of the line current for a wind speed of 11 m/s (THD = 9,26%).

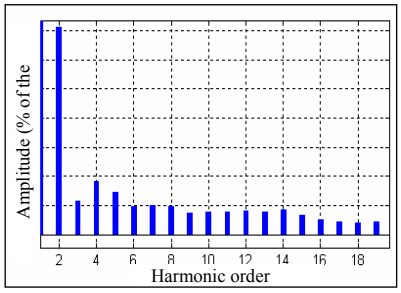

Fig.14. Spectral concentration of the line current starting from the second harmonic for a wind speed of 11 m/s.

In the following part, we will present a strategy of control allowing an active compensation of the harmonics present in the line current.

4.4. Suggestion of a second control strategy for the grid side converter

This converter is controlled in order to provide the reactive component of the current and to compensate the harmonics.

We present the identification method of the harmonic and reactive components by the following block diagram:

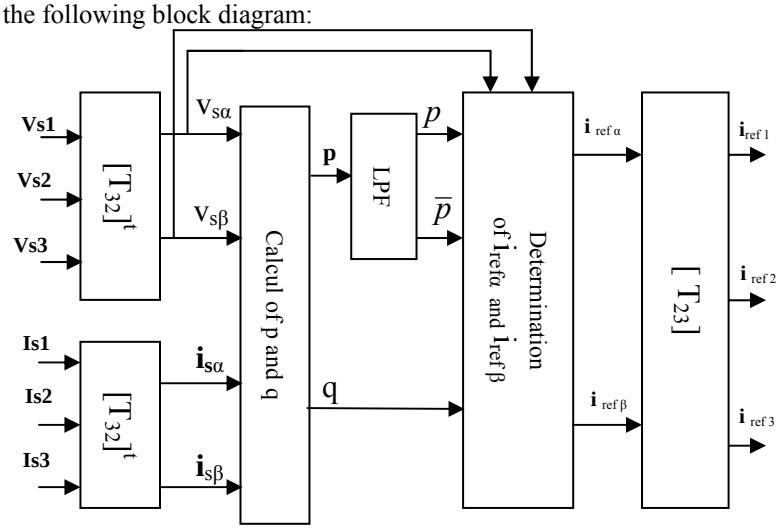

Fig. 15. Harmonic and reactive components identification block diagram.

The three-phase to (α,β) transformation gives the following relations of voltages and currents:

$$\begin{bmatrix} V_{s\alpha} \\ V_{s\beta} \end{bmatrix} = [T_{3/2}]^t \begin{bmatrix} V_{s1} \\ V_{s2} \\ V_{s3} \end{bmatrix} = \frac{2}{3} \begin{bmatrix} 1 & -\frac{1}{2} & -\frac{1}{2} \\ 0 & \frac{\sqrt{3}}{2} & -\frac{\sqrt{3}}{2} \end{bmatrix} \begin{bmatrix} V_{s1} \\ V_{s2} \\ V_{s3} \end{bmatrix} \tag{33}$$

$$\begin{bmatrix} I_{s\alpha} \\ I_{s\beta} \end{bmatrix} = [T_{32}]^t \begin{bmatrix} I_{s1} \\ I_{s2} \\ I_{s3} \end{bmatrix} = \frac{2}{3} \begin{bmatrix} 1 & -\frac{1}{2} & -\frac{1}{2} \\ 0 & \frac{\sqrt{3}}{2} & -\frac{\sqrt{3}}{2} \end{bmatrix} \begin{bmatrix} I_{s1} \\ I_{s2} \\ I_{s3} \end{bmatrix} \tag{34}$$

The instantaneous active power p(t) and the reactive power q(t) are defined by the following relations:

$$p(t) = V_{s\alpha} \cdot I_{s\alpha} + V_{s\beta} \cdot I_{s\beta} \tag{35}$$

$$q(t) = V_{s\alpha} \cdot I_{s\beta} - V_{s\beta} \cdot I_{s\alpha} \tag{36}$$

From the preceding relations we can establish the following expression:

$$\begin{bmatrix} p \\ q \end{bmatrix} = \begin{bmatrix} V_{s\alpha} & V_{s\beta} \\ -V_{s\beta} & V_{s\alpha} \end{bmatrix} \begin{bmatrix} I_{s\alpha} \\ I_{s\beta} \end{bmatrix} \tag{38}$$

The active power p and the reactive power q are respectively made up of a fundamental component active $\overline{p}$ and reactive $\overline{q}$ and of an active harmonic component $\tilde{p}$ and reactive harmonic $\tilde{q}$ such as:

$$\begin{cases} p = \overline{p} + \tilde{p} \\ q = \overline{q} + \tilde{q} \end{cases} \tag{39}$$

A circuit made up of a low pass filter with a comparator can be employed to extract the active harmonic power as shown in the next figure:

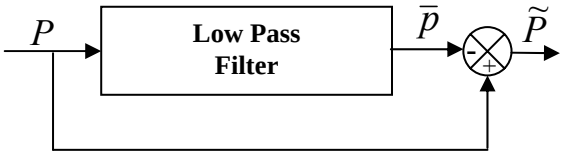

Fig. 16. Extraction of the harmonic power.

The corresponding current components of the harmonic and reactive power are given by the following system:

$$\begin{bmatrix} \tilde{i}_{ref\alpha} \\ \tilde{i}_{ref\beta} \end{bmatrix} = \frac{1}{\Delta} \begin{bmatrix} V_{s\alpha} & V_{s\beta} \\ -V_{s\beta} & V_{s\alpha} \end{bmatrix} \begin{bmatrix} \tilde{p} \\ q \end{bmatrix} \tag{40}$$

With $\Delta = V_{s\alpha}^2 + V_{s\beta}^2$

The C_{grid} current references are expressed as follows:

$$\begin{bmatrix} \tilde{i}_{ref\,1} \\ \tilde{i}_{ref\,2} \\ \tilde{i}_{ref\,3} \end{bmatrix} = \frac{2}{3} \begin{bmatrix} 1 & 0 \\ -\frac{1}{2} & \frac{\sqrt{3}}{2} \\ -\frac{1}{2} & -\frac{\sqrt{3}}{2} \end{bmatrix} \begin{bmatrix} \tilde{i}_{ref\alpha} \\ \tilde{i}_{ref\beta} \end{bmatrix} \tag{41}$$

4.5. Simulation results

For the same wound rotor asynchronous generator and with the second strategy of control of the grid side converter we obtained the following results:

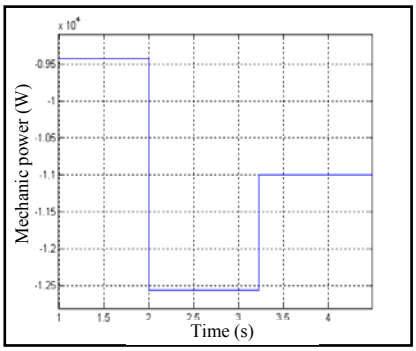

Fig. 17. Mechanical power provided to the rotor of the Doubly Fed Induction Generator.

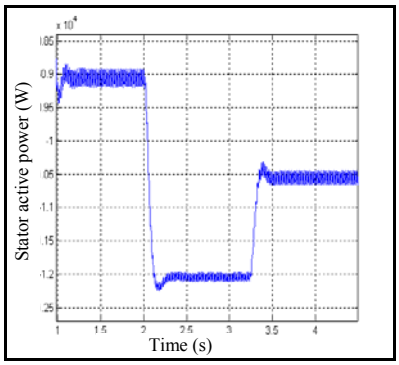

Fig. 20. Stator active power.

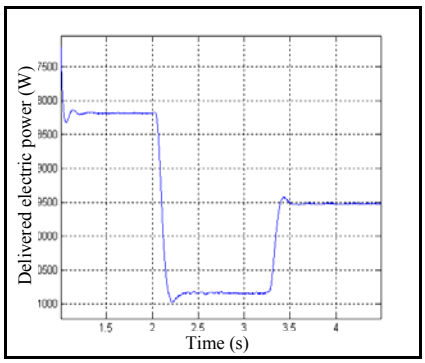

Fig. 18. Power provided to the electric grid.

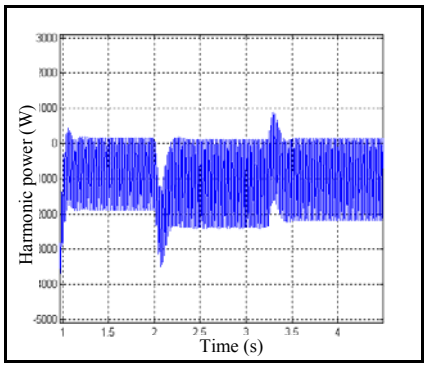

Fig. 21. Harmonic power

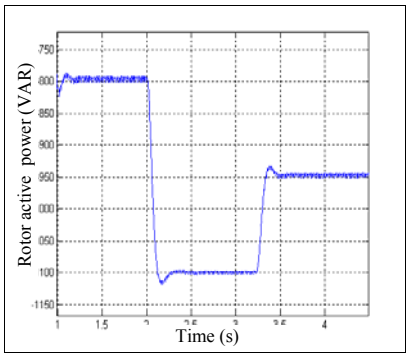

Fig. 19. Rotor active power.

It is noticed well that the undulations in the stator power are eliminated by the C_{Grid} converter; in fact the used control strategy allows compensating the harmonic power. The suggested methodology has clearly improved the quality of power provided to the electric grid.

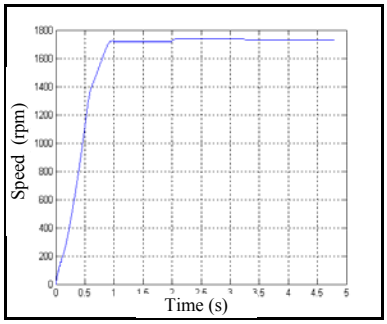

Fig. 22. Rotational speed.

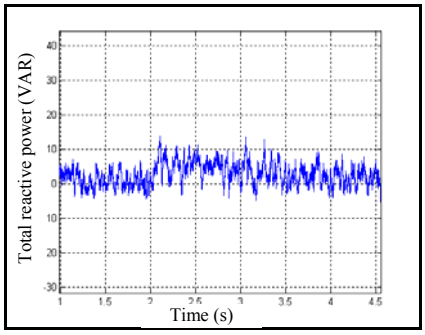

Fig. 24. Global reactive power (grid side).

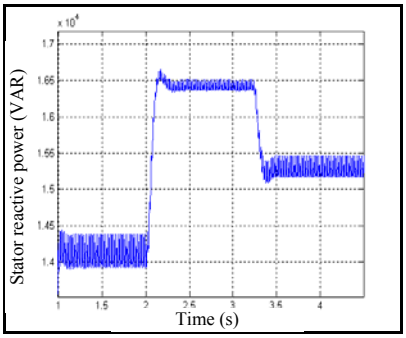

Fig. 23. Reactive power consumed by the generator.

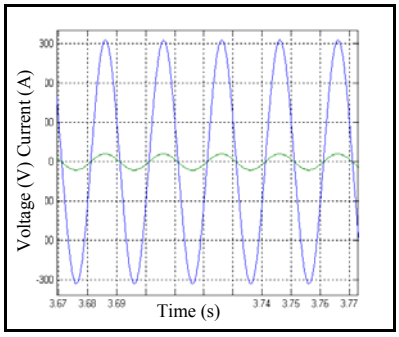

Fig. 25. Line Current and voltage.

The quantity of reactive power consumed by the generator was compensated by the C_{Grid} converter. This converter is controlled by an instantaneous identification of the quantity of consumed reactive power. This method is important for that it compensates not only the necessary part of reactive power; but also enables the harmonics identification and filtering.

5. Conclusion

In this paper we controlled the C_{Grid} converter (grid side converter) by using an instantaneous identification of the reactive power and harmonic. This method makes possible to provide exactly the necessary quantity of reactive power and to compensate the harmonics.

The C_{Rot} converter is used to control the active power provided to the network. a stator flux oriented control strategy is used.

The results obtained are satisfactory and can be improved by using other kinds of regulators (RST, Fuzzy,…). This study could be deeped by testing the robustness of the control under the disturbances of the electric grid.

Appendix:

Induction machine Parameters
Nominal voltage: 220V/380V
Nominal power: 15 kw
Nominal speed: 1480 rpm
Inertia Moment: J = 0.5 kg.m2
Friction coefficient: F = 0.001 N.m/rad/S
A number of poles pairs: Np = 2
Rs = 0.17 Ω
Rr = 0.2 Ω
ls = 5 mH
lr = 5 mH
Lm = 45 mH

6. References

[1] : R. Pena, R. Cardenas, D. Sbarbaro and R. Blasco-Giménez, "variable speed grid connected induction generator for wind energy system", EPE'99 – Lausanne.

[2] : R. Datta and V. T. Ranganathan, "variable-speed wind power generation using doubly fed wound rotor induction machine – a comparison with alternative schemes", IEEE Transaction on power electronics vol.17 NO 3, September 2002.

[3] : S. Bhowmik, J. H.R. Enslin and R. Spée, "performance optimization for doubly fed wind power generation system", IEEE vol.35 NO 4, July/August 1999.

[4] : S. D. Rubira and M. D. McCulloch, "Control method comparison of doubly fed wind generators connected to the grid by asymmetric transmission lines", IEEE Transaction on power electronics vol.36 NO 4, July/August 2000.

[5] : H. Akagi and H. Sato, "Control and performance of a doubly-fed induction machine intended for flywheel energy storage system", IEEE Transaction on power electronics, vol.17 NO 1, January 2002.

[6] : Ion Boldea and Syed Nasar, "The Induction Machine Handbook" by CRC Press LLC 2002

[7] : Hofmann W. and Okafor F., "Doubly-Fed Full-Controlled Induction Wind Generator for optimal power utilization", Conference proceeding PEDS'2001.

[8] : J. L. Rodriguez-Amenedo, S. Arnalte and J. C. Burgos, "Automatic Generation control of a wind farm with variable speed wind turbines", IEEE Transactions on energy conversion, vol.17 NO 2, June 2002.

[9] : Mohamad Alaa Eddin Alali, « Contribution à l'Etude des Compensateurs Actifs des Réseaux Electriques Basse Tension» Thèse de doctorat l'Université Louis Pasteur – Strasbourg I, 2002.

[10] : P. K. S. Khan, J. K. Chatterjee, "Three-Phase Induction Generators, a Discussion on Performance" EMPS, vol. 27, no. 8, 1999.

[11] : B. Hopfensper, D.J.Atkinson, R.A.Lakin "stator-flux-oriented control of a doubly fed induction machine with and without position encoder" IEEE Proc-Electr, Power appl., Vol N° 4 july 2000, pp. 241-250.

[12] : L.H Hansen, F.Blaabjerg, H.C.Christensen, U.lindhart , "Generator and Power Electronics Technology for wind Turbines." Proc. of IECON'2001, pp. 200-205.

[13] : Giuseppe saccomando, Jan Svensson, Ambra Sannino; "Improving voltage disturbance rejection for variable speed wind turbines", IEEE Transaction Energy Conversion,VOL17, No, 3 septembre2002, pp. 422-428.